Single wavelength coarse phasing in segmented telescopes

J.F. Simar,[1,*] Y. Stockman,[1,†] and J. Surdej[2,‡]

[1] *Centre Spatial de Liège, LIEGE Science Park, Avenue du Pré-Aily, 4031 Angleur, Belgium.*

[2] *Bât. B5C, Institut d'Astrophysique et de Géophysique, Université de Liège, Allée du 6 Août 17, 4000 Liège 1, Belgium.*

compiled: February 12, 2015

Space observations of fainter and more distant astronomical objects constantly require telescope primary mirrors with a larger size. The diameter of monolithic primary mirrors is limited to 10 m because of manufacturing limitations. For space telescopes, the primary mirrors are limited to less than 5 m due to fairing capacity. Segmented primary mirrors thus constitute an alternative solution to deal with the steadily increase of the primary mirror size. The optical path difference between the individual segments must be close to zero (few nm) in order to be diffraction limited. We propose in this paper a new inter-segment piston sensor based on coherence measurement of a star image. This sensor is intended to be used in the co-phasing system of future segmented mirrors.

1. Introduction

In order to observe fainter and more distant celestial objects with a better angular resolution, larger telecopes are required to improve the limit of diffraction and the quantity of light collected. Actually, El Gran Telescopio de Canarias (GTC) [1] with a 10.4 m diameter at La Palma Island, is the biggest segmented telescope in the world to be followed by the Thirty Meter Telescope (TMT) [2] at Mauna Kea in Hawaï, the European Extremely Large Telescope (E-ELT) [3] in Paranal and the Giant Magellan Telescope (GMT) [4] in Las Campanas, all planned to be in operation sometimes during the next decade.

The optical path difference (OPD) between segments in such mirrors must be reduced nearly to zero (the segments must be co-phased) depending on the spectral requirements, in order to be diffraction limited over the whole aperture. In the visible spectral range, this distance must be typically below 10 nm. The initial OPD (before co-phasing system is turned ON) in segmented telescopes is typically about 100 μm because of mechanical structure tolerance. Then, two measurement sensors (coarse and fine) must be used in order to correct from 100 μm to 10 nm OPDs. Fine measurement techniques as described in [5] and [6] have been studied. Also, two well known coarse measurement techniques have been evaluated, the Multi-spectral piston sensor [7] and the Broadband phasing algorithm [8]. These have been considered as a baseline for this work. In the present paper, we propose a new concept, capable to measure OPD between 0 μm and 200 μm at a relatively low cost and with less stringent mass constraints in comparison with other techniques.

1.A. Broadband phasing algorithm

This technique involves some broadband input light and measuring the coherence degree of the transmitted light. This light has a coherence length (L_c) that limits the range of possible measurement. This length, so-called coherence length, is given by (see [8]):

$$L_c = \frac{\lambda^2}{2\Delta\lambda} \tag{1}$$

where λ is the central wavelength and $\Delta\lambda$ is the bandwidth of the filter. The degree of coherence, defined as the normalized correlation of the electric fields, is related to the OPD as a Gaussian function of the distance between segments. Note the factor of 2 in Eq. (1) denominator: it comes from the input light reflection on the main mirror, giving an OPD equal to twice the distance between segments.

* Corresponding author: jfsimar@ulg.ac.be

† Corresponding author: ystockman@ulg.ac.be

‡ Corresponding author: jsurdej@ulg.ac.be

2. Proposition

We propose here a new coarse phasing method involving the measure of the degree of coherence of the reflected light. It uses the Point Spread Function (PSF) of a star in the field of view (FOV) of the telescope. This PSF is generated by a sub-pupil configuration that can be adapted for any segmented telescope. For the purpose of demonstration, we used a three segment telescope with the sub-pupil configuration depicted in Fig 1.

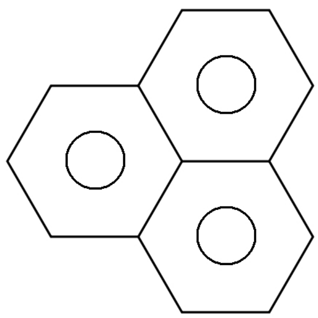

Fig. 1. Telescope segments (hexagons) and sub-pupil (circles) configuration

The input coherent star light is reflected by the main mirror of the telescope and after passing through a mask with the sub-pupil configuration, the light is focused on a CCD where the PSF is recorded. This image, is equivalent to the square modulus of the Fourier Transform of the sub-pupil configuration [9]. After registration, the Inverse Fourier Transform is performed for the CCD image (PSF). This mathematical operation gives the Optical Transfer Function (OTF) which is composed of the Modulation and Phase Transfer functions (MTF and PTF respectively). Finally, measuring the different heights of the MTF peaks gives the OPD between the different segments. We will present the experimental setup and some results, the co-phasing probability (in a specific direction of the sky) and advantages and limitations of this method in the next sections.

This system is based on Fourier Optics [10]. Here, the PSF is formed by the interference of light in the image plane of the telescope. We can define the electric field in the sub-pupil plane by:

$$E(x, y) = A(x, y) \cdot e^{i \cdot OPD(x,y) \cdot \frac{2\pi}{\lambda}} \tag{2}$$

where (x, y) are the coordinates in the sub-pupil plane. When the coherent light (star light) impinges the telescope, it is reflected several times and finally reaches a CCD sensor placed in the image plane. This PSF is defined as:

$$PSF(u, v) = |(FT(E(x, y)))|^2 \tag{3}$$

$$PSF(u, v) = |(FT(A(x, y) \cdot e^{i \cdot OPD(x,y) \cdot \frac{2\pi}{\lambda}}))|^2 \tag{4}$$

where FT is the Fourier Transform and (u, v) are the spatial frequency coordinates in the image plane. When we apply the Inverse Fourier Transform on the acquired CCD PSF, we obtain the OTF. OTF is a complex number, that is composed of an amplitude and phase. The PTF gives several information about the OPD of sub-pupils when it is in the $(-\lambda/2, +\lambda/2)$ range including Piston, Tip/Tilt and higher order aberrations, but recent experimental results show that the MTF also gives information about the OPD when it is in the range of the coherence length of the filter (Eq. (1)). The method which exploits these results and leads to the measurement of the OPD (Piston only), is described hereunder. Tip/Tilt and higher order aberrations are not concerned by this paper.

2.A. Theory

The MTF is the amplitude part of the OTF, and is given by:

$$MTF(x, y) = |FT^{-1}(PSF(u, v))| \tag{5}$$

where (x, y) are the MTF coordinates. In the MTF, the heights of the surrounding peaks (not the central peak), are related to the coherence degree of the PSF, and the coherence degree is related to the OPD. Thus, by measuring the height of the MTF surrounding peaks, we can retrieve the OPD between the segments. Figure 2 shows a simulation of different MTF for various PSF and a spectral filter centered at $\lambda = 632.8$ nm with $\Delta\lambda = 1$ nm: we see that when the OPD is null, the fringe contrast is 1 and that the MTF peaks are maximum, but as the OPD increases, the MTF peaks become smaller and smaller, until they completely disappear. We put the OPD in abscissa and the MTF peaks height in ordinates and fitted it with Gaussian, Cardinal sinus (Sinc), Linear and Parabola functions, and the best fitted function was the Gaussian function.

According to the fitting procedure, the MTF normalized peak heights (MTF_{nph}), are related to the OPD by means of the following Gaussian relation:

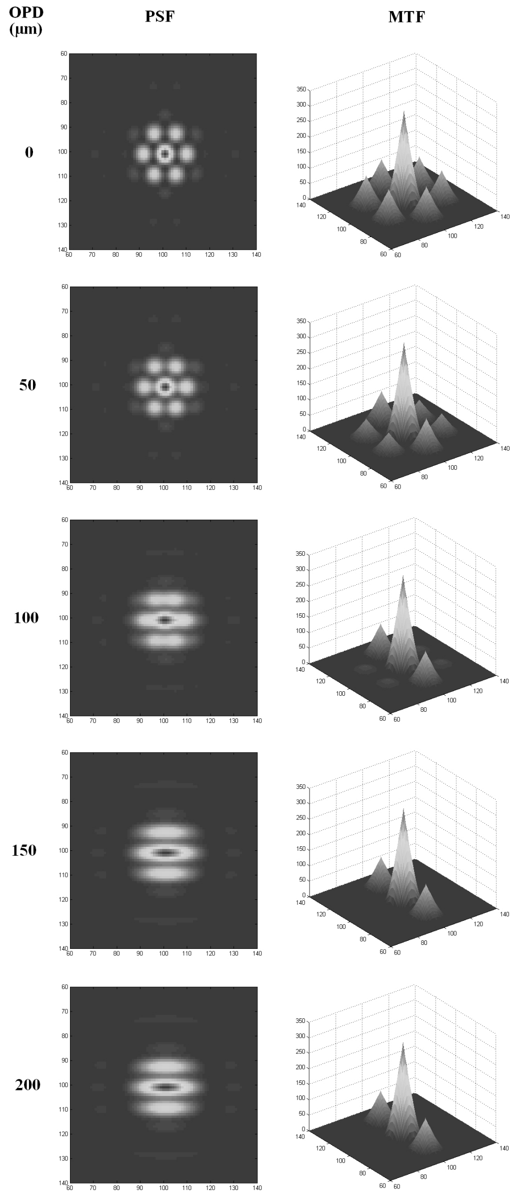

Fig. 2. Simulation of the PSF (left column) and MTF (right column) for a spectral filter centered at $\lambda = 632.8$ nm with $\Delta\lambda = 1$ nm for different OPD values of a single pupil

$$MTF_{nph} = e^{-\left(\frac{OPD}{PAR}\right)^2} \tag{6}$$

where PAR is a fitting parameter. Then, the OPD is merely given by:

$$OPD = PAR \cdot \sqrt{-\ln(MTF_{nph})} \tag{7}$$

Note that the MTF central peak height (MTF_{cph}) is always the same regardless the coherence degree, the MTF_{cph} is too the cross correlation of all sub-pupils [9], so its height is the maximum height of a single peak multiplied by the number of sub-pupils and is given by:

$$MTF_{cph} = max_{ph} \cdot n \tag{8}$$

where max_{ph} is the maximum surrounding peak height and n is the number of sub-pupils. Then, the expression of MTF_{nph} is given by:

$$MTF_{nph} = \frac{MTF_{ph}}{max_{ph}} \tag{9}$$

and following Eqs. (8) and (9):

$$MTF_{nph} = \frac{MTF_{ph}}{MTF_{cph}} \cdot n \tag{10}$$

where MTF_{ph} is the non-normalized surrounding peak height.

Finally, using Eqs. (7) and (10), we obtain:

$$OPD = PAR \cdot \sqrt{-\ln\left(\frac{MTF_{ph}}{MTF_{cph}} \cdot n\right)} \tag{11}$$

This equation gives the OPD in terms of the fitting parameter, the surrounding peak height, the central peak height and the number of sub-pupils. The OPD is thus not sensitive to the input light power because if the light power changes, the surrounding and the central peaks also change in the same proportion, and thus, the resulting OPD remains the same.

We define $MTF_{nph} = 0.5$ when the OPD is equal to $0.5L_c$, then, PAR is given by:

$$PAR = \frac{0.5L_c}{\sqrt{-\ln 0.5}} \tag{12}$$

Remember that L_c depends on the bandwidth of the input spectrum. Thus, for the data simulated in Fig. 2, $PAR = 120.24$ µm.

3. Experimental results

3.A. Optical setup

Figure 3 shows the optical demonstration bench used for this experiment.

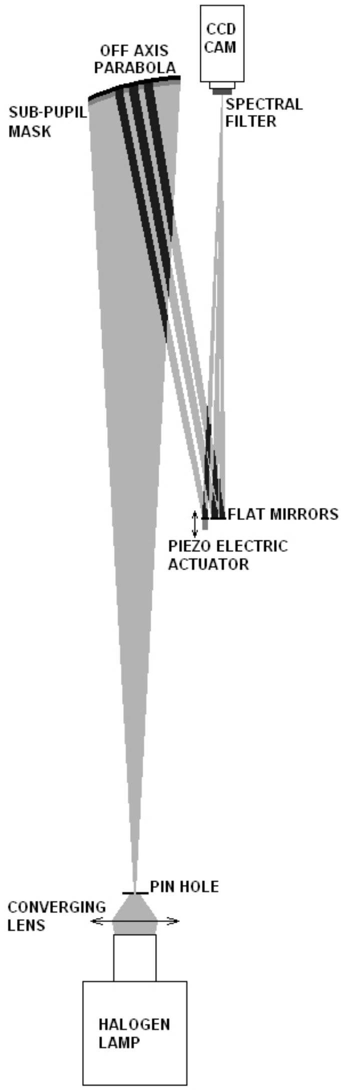

Fig. 3. Optical demonstration bench

Optical setup components
- Halogen lamp (250W bulb)
- Converging lens
- Pin Hole (20 μm diameter)
- Off axis parabola (10 cm diameter)
- Sub-pupil mask (3 holes of 8 mm diameter each one)
- Flat mirrors
- Piezo electric actuator (400 μm displacement)
- Spectral filter ($\lambda = 632.8$ nm, $BandWidth = 1$ nm)
- CCD Camera (AVT Pike F-032B)

Table 1. Optical setup components

3.A.1. Components

The optical setup was elaborated with the components in the table 1.

A halogen lamp, a converging lens and a pin hole simulate a star. An off-axis parabola simulates a telescope's main mirror and the sub-pupil mask serves as the telescope's sampling mask (sub-pupil). The mirrors and a single piezo electric actuator are used to introduce a known piston error and the image filtered by the spectral filter is recorded by the CCD camera in the focal plane.

3.A.2. Optical Setup Explanation

When the light coming from a star (pin hole) impinges the off-axis parabola, it is reflected and converges on the CCD (focal plane), reflected by the mirrors equipped with a single piezo electric actuator. The CCD recorded image is the PSF of the sub-pupil configuration deformed by a known piston error (introduced by the piezo electric actuator) and filtered. Then, mathematically, the inverse fast Fourier transform (IFFT) is performed over the PSF in order to obtain the OTF, and finally, analyzing the heights of the MTF, we retrieve the OPD between the actuated mirror and the non actuated mirrors of the parabola.

3.B. Measurements

Table 2 and Fig. 4 summarize a set of piston measurements, performed with the optical bench in order to estimate the measurement errors.

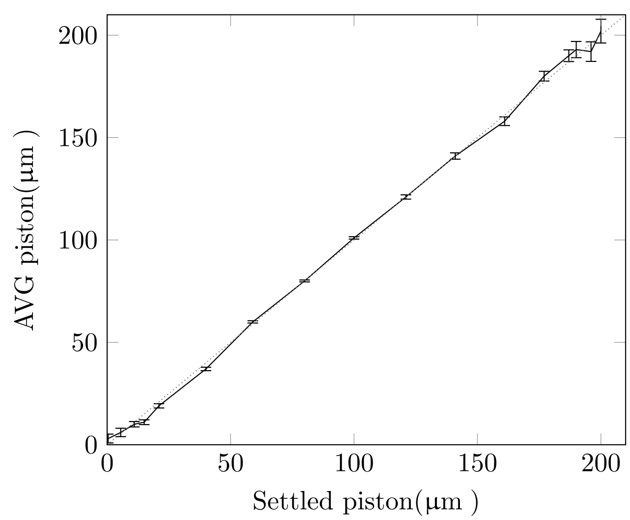

Fig. 4. Graphic representation of sets of optical bench measurements

Settled piston (nm)	AVG (nm)	Difference (%)	Standard dev (nm (%))
412	3027	634,71	720 (23,79)
5465	5995	9,70	683 (11,39)
10877	9831	-9,62	437 (4,45)
15129	11349	-24,99	392 (3,45)
20622	18541	-10,09	347 (1,87)
40200	37105	-7,70	279 (0,75)
59487	60088	1,01	184 (0,31)
79945	80184	0,30	158 (0,20)
99992	100791	0,80	191 (0,19)
120659	120717	0,05	348 (0,29)
140994	141412	0,30	515 (0,36)
161163	158457	-1,68	701 (0,44)
177285	180081	1,58	792 (0,44)
186920	190299	1,81	954 (0,50)
190235	193032	1,47	1319 (0,68)
195518	192418	-1,59	1593 (0,83)
200391	201864	0,74	1932 (0,96)

Table 2. Set of optical bench measurements, settled piston (first column), average measured piston (second column), difference (AVG compared to settled piston) (third column), and measured standard deviation (fourth column)

3.B.1. Measurement Analysis

In Table 2 and Fig. 4 we observe that the Difference (Accuracy) and the Standard Deviation (Stability) are degraded at the extremes of the measurement range. It is due to the Gaussian shape of the signal.

In Fig. 4, there is a dotted curve (piston without errors) and a solid curve (measured piston), the differences between them are the Measurement Errors. The coherence of the signal is Gaussian (as a function of the distance between the segments). At the extremes of the range the non linearities of the Gaussian become more important and then the method gets more unstable. That is to say that for the same measurement error over the whole measurement range and after application of Eq. (11), we obtain an error increase at the extremes of the measurement range. This effect has been simulated in Fig. 5 where we can observe the distance error and how this error is amplified.

The Fig. 5 is the graphic representation of the equation $|F(MTF_{nph}) - F(MTF_{nph} - errorMTF_{nph})|$ where F is the Eq. (7), and $errorMTF_{nph}$ is a constant value over the whole measurement range.

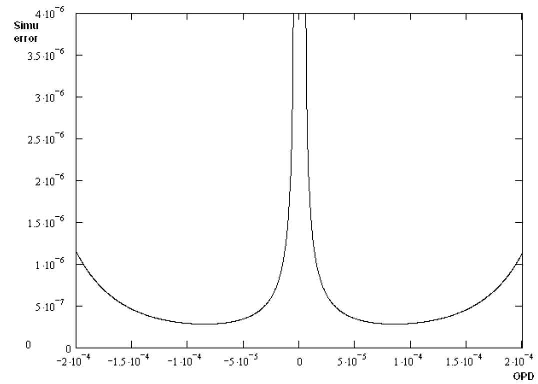

Fig. 5. Error amplification effect: in abscissa the settled piston (m) and in ordinates the simulated error (m)

The error seems to be infinite at OPD near to 0, because the Eq. (7) is undefined (complex solution) for MTF_{nph} values bigger than 1 ($OPD = 0$ when $MTF_{nph} = 1$).

This error can be reduced by performing more measurements and averaging them.

4. Co-phasing probability

In order to realize the co-phasing task, it is mandatory to have a sufficiently bright star that the telescope can detect. The apparent magnitude (M_v) of the required star has to be calculated. The computation indicates that for our camera sensitivity and GTC and E-ELT telescope, the required M_v must be brighter than 15 for GTC and 12 for E-ELT for a coherence diameter of 12 cm (normally at all observation places chosen for big telescopes) with 10 min of integration time. In order to find the probability to find such stars, we used a stellar population algorithm depending on, the field of view (FOV), direction (galactic coordinates) and observation band. This probability is the probability to achieve the co-phasing in the specified direction. Table 3 shows different probabilities calculated for $FOV = 15'$ (GTC), $FOV = 5'$ (E-ELT), $Band = R$ and $BW = 10$ nm for different galactic coordinates. This study has been carried out in order to verify that this method can be implemented with actual segmented mirror sizes and sensitivities. For a TMT, E-ELT or any other future giant telescope, this would mean that the probability of finding a sufficiently bright star would be near from 100% but due to the FOV smaller than $15'$ (e.g. E-ELT), the telescope will shall be directed towards a known position with a sufficiently bright star.

Lon (°)	Lat (°)	GTC Prob	E-ELT Prob
30	0	1	0.9850
60	0	1	0.9474
135	0	1	0.7406
180	0	1	0.6909
0	10	1	0.7804
30	10	1	0.7305
60	10	1	0.6556
90	10	1	0.5763
135	10	1	0.4877
180	10	1	0.4553
0	30	1	0.2705
30	30	1	0.2587
60	30	1	0.2387
90	30	1	0.2184
135	30	1	0.1957
180	30	1	0.1888
30	60	0.9974	0.1194
60	60	0.9964	0.1159
90	60	0.9948	0.1116
135	60	0.9919	0.1063
180	60	0.9904	0.1042
90	90	0.9775	0.0916

Table 3. Co-phasing success probability for the GTC (FOV = 15') [1] and the E-ELT (FOV = 5') [3] telescopes and the sensitivity of an AVT Pike F-032B camera

5. Advantages and limitations

5.A. Advantages

- This method is not perturbed by the segment edges.

- By combining this method with two wavelength equations (see [11]) and the method described in [5], it is possible to perform the whole co-phasing task from 200 μm down to 10 nm with two spectral filters and one optical setup.

- This method uses one Fast Fourier transform (FFT) and some arithmetic functions, and therefore requires modest computer performances.

- It is a lightweight optical setup (one mask, two spectral filters, one shutter and one CCD camera, to perform the whole co-phasing task).

- The optical setup is separated from the main optical path, then, the mirrors are not manipulated during the mounting of the sensor.

- No laser source is required. Mass, cost and temperature performances are better in comparison to laser systems.

5.B. Limitations

- The precision of this method is limited, but when combining with [11] and [5] the whole co-phasing task can be performed.

- The co-phasing capability depends on the star brightness and the CCD sensitivity. It is limited by the field of view of the telescope. This limitation can be overcome by changing the sub-pupil size or redirecting the telescope to a known star coordinate.

6. Conclusions

- This method maximizes the OPD measurement range because it uses the whole coherence length of the filter. It measures the absolute piston value instead of differential piston values.

- This method does not perturb the telescope main mirror, is easier to mount than capacitive methods, and can be easily combined with similar fine measure techniques in order to achieve the whole co-phasing task.

7. Acknowledgments

This work has been supported by Centre Spatial de Liège and financed by the University of Liège. The authors acknowledge support from the Communauté française de Belgique - Actions de recherche concertées - Académie universitaire Wallonie - Europe.

References

[1] GTC Website, http://www.gtc.iac.es/
[2] TMT Website, http://www.tmt.org/
[3] E-ELT Website, http://www.eso.org/
[4] GMT Website, http://www.gmto.org/
[5] Géraldine Guerri, Steeve Roose, Yvan Stockman, Alexandra Mazzoli, Jean Surdej, Jean-Marc Defise. First steps of the development of a piston sensor for large aperture space telescopes. *SPIE*, vol. 7731, p 165 (2010).
[6] Fabien Baron, Isabelle Mocoeur, Frédéric Cassaing, Laurent M. Mugnier. Unambiguous phase retrieval as a cophasing sensor for phased array telescopes. *J. Opt. Soc. Am. A.*, 1000, Vol. 25, No. 5, May 2008.

[7] François Hénault. Multi-spectral piston sensor for co-phasing giant segmented mirrors and multi-aperture interferometric arrays. *J. Opt. A: Pure Appl. Opt.*, 11 125503, 2009.

[8] G. Chanan, M. Troy, F. Dekens, S. Michaels, J. Nelson, T. Mast, and D. Kirkman. Phasing the Mirror Segments of the Keck Telescopes: The Broadband Phasing Algorithm. *Appl. Opt.*, 37(1):140-155, 1998.

[9] Sebastien Van Loo, Etude de Senseurs de Front d'Onde Apliqués à la Synthèse d'Ouverture Optique pour la mesure du Piston et du Tilt, *Université de Liège*, (05/2003).

[10] Eugene Hecht, *Optics*, Pearson Education, Inc., p 519 (2002).

[11] C. R. Tilford, Analytical procedure for determining lengths from fractional fringes, *Appl. Opt.*. vol. 16, p 1857-1860 (1977).